Dynamic Soliton-Like Modes

Ming-Feng Shih* and Fang-Wen Sheu
Department of Physics, National Taiwan University, Taipei 106, Taiwan
(Received 11 October 2000)

Incoherent optical spatial solitons require noninstantaneous nonlinearity, i.e., the local intensity fluctuation of the solitons must be faster than the medium can respond. Observing partially incoherent bicomponent solitons, we find that there exists a threshold speed. When the fluctuation of the soliton intensity, resulting from the time-varying interference of its constituent modes, is below the threshold, the soliton beam and its induced waveguide oscillate violently. Just above the threshold, the soliton-induced waveguide is observed to be dragged by the soliton beam.

DOI: 10.1103/PhysRevLett.86.2281 PACS numbers: 42.65.Tg, 42.65.Sf

An optical spatial soliton [1] is an optical beam that does not diffract due to the exact compensation from the self-focusing effect originating from the beam's nonlinear interaction with the medium. It can also be viewed [2] as an optical beam that generates an optical waveguide via the medium nonlinearity, and the beam itself is the guided mode of this induced waveguide. When the light beam is the fundamental mode of its induced waveguide, the soliton is of the bright type, and, when the light beam is the second mode at cutoff, the soliton is of the dark type. In either case, the solitons are solely coherent entities, meaning that the phase difference between any two separated points is entirely predictable.

Spatially incoherent optical spatial solitons [3–8] have attracted much research interest. To observe the spatially incoherent solitons, the nonlinearity must be "noninstantaneous." In a loose definition, it means the nonlinear response of medium is slow enough that it cannot respond to the relatively rapid local intensity fluctuation of the optical beam. The medium can only "see" the light intensity averaged over a period of time. In one analysis [4] for partially incoherent solitons that adopts the linear waveguide approach, it decomposes the solitons into the modes of its induced waveguide, and the relative phases between different modes are quickly randomly varying. The local intensity of the beam is therefore fluctuating fast due to the varying random interferences of the constitutive modes. This averages, in the order of the material response time, to a smooth intensity profile, which via the material nonlinearity generates a spatially smooth and temporally constant waveguide that can accommodate all the constitutive modes of the soliton beam. Now the questions arise: How fast should the local intensity fluctuate to make the nonlinearity of the medium look noninstantaneous in order to form incoherent solitons? What happens to the incoherent solitons if the intensity fluctuation is not fast enough?

To target such problems for the first time, we start the study experimentally with the multicomponent solitons [4] in the photorefractive strontium barium niobate (SBN:60) crystal. The nonlinearity is of the saturable type that can support multicomponent solitons, and its noninstantaneous response speed is proportional to the optical intensity [9]. The multicomponent solitons, belonging to the least complex category of the spatially partially incoherent solitons, are composed of only the fundamental and the second modes. The intensity fluctuation of the bicomponent soliton beam is controlled by varying the relative phase between the two constituent modes. We find that, when the varying speed of the relative phase as well as the intensity fluctuation is much above a certain threshold, the medium looks noninstantaneous, and the partially incoherent optical spatial solitons form. However, as the speed of the intensity fluctuation is gradually reduced to be just above the threshold, we observe that the soliton beam and its induced waveguide move in a spatially and temporally dynamic motion, in which the waveguide lags to the soliton beam. When the intensity fluctuation speed is further reduced to be below the threshold, the soliton beam and its induced waveguide begin to oscillate violently in the medium. We name these soliton phenomena as "dynamic soliton-like modes." Although we experiment on the bicomponent solitons, we believe such threshold behaviors may exist for other partially incoherent optical solitons [3] and be related to the modulation instability of partially incoherent light [10].

Intuitively, one may understand why there is a threshold: The noninstantaneous medium takes the time-average intensity to yield its nonlinear index change, which is *constant* if the intensity fluctuation due to the interference of the two modes is too fast for the medium to respond. When the varying speed of the relative phase between the two modes is gradually reduced, the speed of the intensity fluctuation is also reduced. As a result, the medium can gradually respond and yield a *time-varying* index perturbation as compared to the constant index change. The magnitude of the time-varying index perturbation also becomes larger as the speed of the intensity fluctuation becomes slower. At the beginning, when the intensity fluctuation is relatively fast and the index perturbation is very small, the soliton beam can fine-adjust and reshape itself due to the robustness of the stable soliton. As the intensity fluctuation becomes slower and the index perturbation becomes larger, at some point, the soliton beam can no longer adjust itself to its stationary soliton

0031-9007/01/86(11)/2281(4)$15.00

shape. At this point, the induced waveguide also fluctuates as the light beam does. This fluctuating waveguide will further affect the light beam later coming into the medium and then affect more the waveguide itself. With such a feedback manner, it is not a surprise that there exists a critical or threshold point. This intuition is proved to be true by the beam propagation simulation.

The experimental setup shown in Fig. 1 is similar to that in Ref. [4]. We split the TEM_{00} extraordinarily polarized soliton beam, whose wavelength is 532 nm, into two beams, A and B, with powers of 2.4 and 1.4 μW, respectively. We let B pass through the edge of a piece of thin glass tilted at a proper angle to make B similar to a TEM_{10} mode. B is then reflected by a mirror positioned by a piezocrystal powered by a function generator set at a few hundred Hz. The optical path of B is oscillating back and forth about one wavelength. We superimpose A and B, which act as the source for observing the bicomponent soliton. We then focus $A + B$ [A and B shown in Figs. 2(a) and 2(b), respectively, as the other being blocked] by a lens and have the minimum beam waist located at the input face of a 5-mm-long SBN:60 crystal ($n = 2.35$ and $r_{33} = 234$ pm/V). The minimum beam waist (FWHM, full width at half maximum) of A is about 13 μm. We also focus a probe beam C of wavelength at 633 nm into the crystal at the same spot to help observe the waveguide induced by the solitons [Fig. 2(c)]. We need not worry about C to perturb the soliton-induced waveguide since it is at a much less photosensitive wavelength and with its intensity about 15% of that of $A + B$ [11]. An ordinarily polarized uniform light beam covers the entire crystal for background illumination. The intensity ratio between the peak intensity of $A + B$ and the background illumination is about eight [9]. We then use a translating lens plus a charge-coupled device (CCD) camera to observe the beams at the input and output faces of the crystal. Without applying voltage ($V = 0$) across the crystal, both $A + B$ and C naturally diffract [Figs. 2(d) and 2(e)]. When a field 2000 V/cm is applied on the crystal, the soliton forms [Fig. 2(f)] in a few seconds. We take the picture of A (B) immediately after B (A) is blocked. Figures 2(g) and 2(h) at the output face of the crystal show that $A + B$ is indeed a bicomponent soliton, and Fig. 2(i) (taken when $A + B$ is filtered out) shows that C is guided well by the soliton-induced waveguide. In the following experiment, we use a prism in front of the CCD camera to separate C from $A + B$ in order to observe $A + B$ and C simultaneously.

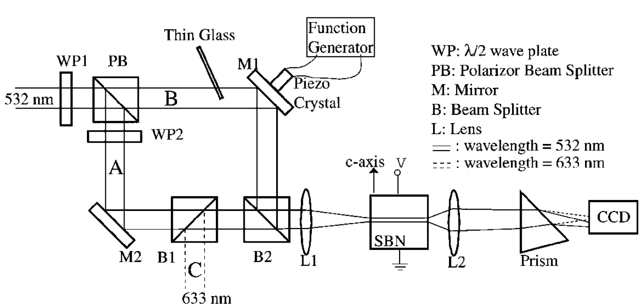

FIG. 1. The experimental setup.

When the frequency of the function generator is reduced to about a few Hz, at the input face of the crystal, we begin to see the oscillation behavior [12] of the soliton beam $A + B$, which is about 6 to 8 μm from one extreme point to the other extreme point (all the following oscillations are measured in the similar way) at the input. The oscillation comes from the interference of A and B. The center of the beam goes to the left(right) when A is in phase with the left(right) lobe of B [Fig. 3(a)]. The oscillation of $A + B$ of similar amplitude is also observed at the output face of the crystal. Nevertheless, at this frequency, probe beam C does not oscillate (or move within the measurement error about 2 μm). We therefore conclude that the nonlinear response "seen" by the varying beam $A + B$ is noninstantaneous and this nonlinearity yields a constant waveguide. Since A and B at the input face of the crystal are close to the modes of their induced waveguide and are the eigenmodes at the output face, their interference pattern should vary in a similar way at both faces. This is why we observe similar oscillation amplitudes of $A + B$ at the input and output planes. Notice that $A + B$ curves right and left in the crystal because A (the fundamental mode) and B (the second mode) differ in phase velocities. At intensity ratio equal to eight, the effective indices [13] of A and B differ about two-fifths of the total index change induced by the externally applied electric field. The effective index difference is therefore about $\frac{2}{5} \times \frac{1}{2}(2.35)^3(234 \times 10^{12})(2 \times 10^5) = 0.000\,12$, which yields about one plus cycle of the right-and-left oscillation of the superimposed beam $A + B$ during the 5-mm propagation in the crystal.

We further reduce the frequency of the function generator. At about 500 mHz, the oscillation amplitude of $A + B$ at the output face increases to about 11 μm [Fig. 4(a), dashed curve]; at the same time the oscillation amplitude

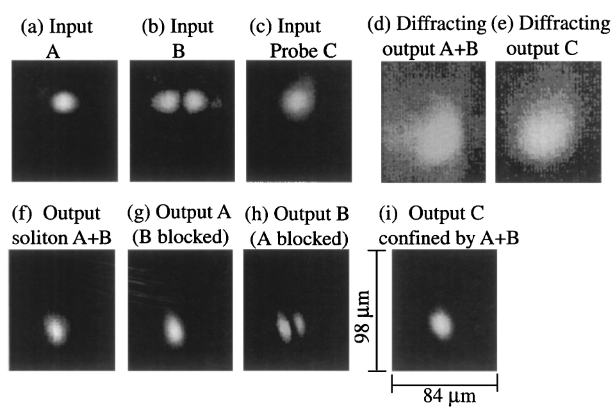

FIG. 2. (a)–(c) The fundamental mode A, the second mode B, and the probe beam C at the input face of the crystal. (d)–(e) The pictures of their natural diffractions at the output face of the crystal. The pictures of the bicomponent soliton $A + B$ (f), its constituent components A (g) and B (h), and the confined probe C (i) at the output face of the crystal when the soliton forms.

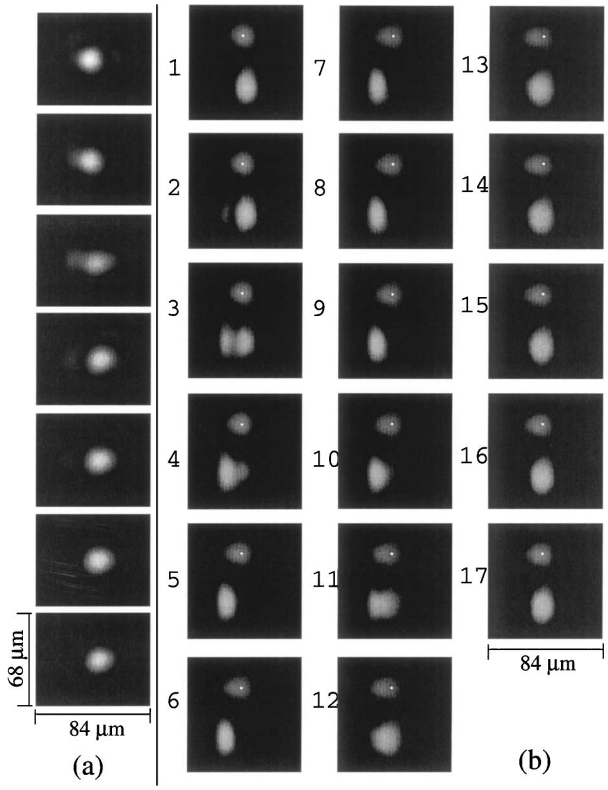

FIG. 3. (a) The oscillation of $A + B$ at the input face of the crystal. (b) The oscillations of $A + B$ and C at the output face of the crystal. The white dots in each picture are added manually to mark the same point on the CCD camera. This is for an easy reference of the position of the probe C. Because of the dispersion caused by the prism, the vertical scale is not available.

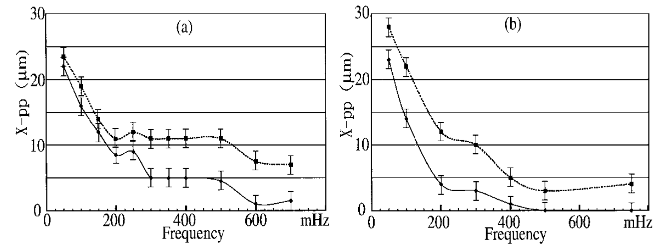

FIG. 4. The oscillation amplitudes, measured from the two extreme points, of the soliton beam $A + B$ (dashed curves) and the probe C (solid curves) at the output face of the crystal vs the frequency of the function generator for two sets of light intensities specified in the text.

of the probe C begins to be observable at about 5 μm [Fig. 4(a), solid curve]. This indeed indicates that at this frequency the material can somewhat respond to the varying intensity of $A + B$, the nonlinearity is no longer noninstantaneous, and the soliton-induced waveguide is not constant. Another interesting observation is that the movement of the soliton-induced waveguide lags behind the movement of the soliton beam. It is shown in pictures 1 to 4 of Fig. 3(b) (at the output face, each picture taken at 0.14 s apart), in which the soliton beam $A + B$ (the lower bright spot) has already moved to the leftmost position and the probe beam C (the upper bright spot) is just about to move left, and, shown in pictures 9 to 12, $A + B$ moves right before C moves right. Since the time-varying wiggly moving soliton light beam still keeps its well self-trapped shape, as does the probe beam confined by its induced waveguide, we therefore name this phenomenon as a dynamic soliton-like mode. Notice that this spatially and temporally dynamic soliton-like mode is one-dimensionally more complicated than the "dynamic spatial solitons," which have only spatial dynamics along the propagation direction [14].

We further reduce the frequency of the function generator. In the frequency range between 500 and 300 mHz, we do not observe significant increase of the oscillation amplitudes of $A + B$ and C at the output face but observe only the lagging of the movement of C compared to that of $A + B$ is gradually reduced. As the frequency is below the threshold of 200 mHz, we observe that oscillations of $A + B$ and C at the output face of the crystal increase significantly as the frequency of the function generator is reduced [Fig. 4(a)]. At the same time, $A + B$ and C move to their respective extreme positions *synchronously*. When the frequency is very low (Fig. 4), both the swinging amplitudes of $A + B$ and C at the output face of the crystal are much larger than that of $A + B$ at the input. As the limit of our function generator is about 50 mHz, we cannot observe the behavior of the dynamic soliton-like modes with even smaller oscillation frequency. In another experiment with the power of every beam reduced to half [Fig. 4(b)], the curves are corresponding scaled to half in the frequency coordinate since the speed of the photorefractive response is proportional to intensity.

In the $(1 + 1)$-dimensional simplified beam propagation simulation, the saturable nonlinear refractive index everywhere in the medium is described by

$$\left(\tau \frac{\partial}{\partial t} + 1\right)\delta n = -\gamma \frac{1}{1 + |A + B|^2}, \qquad (1)$$

where τ is the relaxation time of the refractive index, and γ is the nonlinear coefficient required to form the bicomponent soliton. The beam size (FWHM) is equal to 12 μm, and the crystal length is equal to 5 mm. We do not include the diffusion effect that causes the solitons to self-bend [15]. At the input face, A is set at zero phase and B is set at an initial phase $2\pi t/T$, where $T = 1/f$ is the period of the function generator. The simulation is repeated to run with each time step equal to $T/24$. Within every time step, the light beam from the input face to the output face is calculated by the beam propagation algorithm [16] with the relaxed refractive index that is based on the intensity obtained in all past time steps. To reach the steady state, that is, when the light beam and its induced waveguide repeat themselves every 24 time steps, requires running the propagation for at least 1200 time steps or iterations [17]. The results of the simulation are shown in Fig. 5(a) for different ratios of τ/T from 2 to 80. At $\tau/T = 40$ [Fig. 5(d)] or larger ratio, we observe

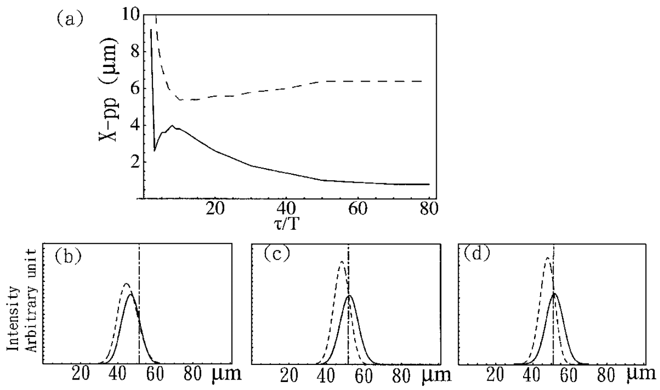

FIG. 5. (a) The oscillation amplitudes of the soliton beam $A + B$ (dashed curve) and its induced waveguide (solid curve) after 5-mm propagation. The beam profiles of the bicomponent soliton (dashed curve) and the probe beam (solid curve) guided by the induced waveguide for (b) $\tau/T = 2$, (c) $\tau/T = 6$, and (d) $\tau/T = 40$. The dotted line is the center of the oscillation.

that the soliton beam stabilizes itself by a negative feedback mechanism. Whenever there is a perturbation of the induced waveguide, it goes in the opposite direction of the soliton beam. This prevents the soliton beam from going further right or further left and bends the soliton back to its central track. For τ/T between 30 and 3 [Fig. 5(c)], the soliton beam $A + B$ and its induced waveguide no longer oscillate oppositely. This is what we observe in the experiment: There is a time delay between the motion of the induced waveguide and that of the soliton beam. Notice that, at these τ/T ratios, the simulation shows that the oscillation amplitude of the induced waveguide increases to a plateau [Fig. 5(a), solid curve] just as the situation we observe in the experiment but the oscillation amplitude of the soliton $A + B$ does not [Fig. 5(a), dashed curve]. This is because, in the simulation, the soliton beam oscillates in the medium and forms nodes. If the length of the observation window is close to the nodes, we observed decreased oscillation amplitudes; otherwise, we observe increased amplitudes. Because of the fact that the simulation is one dimensional and the soliton in the experiment is two dimensional, we expect the nodes to appear at different lengths. At $\tau/T = 2$ [Fig. 5(b)] or lower, the simulation shows that the soliton beam and its induced waveguide oscillate in the same direction. When τ/T is below the threshold about 2 to 3, this positive feedback causes the beam to oscillate violently. Nevertheless, the beam still keeps its well confined shape within 5 mm of propagation; therefore we call it a soliton-like mode in contrast to a diffracting beam. If we let the beam keep propagating a longer distance, the oscillation amplitude grows up, and finally the beam breaks up. The distance the beam can propagate before it breaks up depends on the τ/T ratio. We point out that, from this point of view of the interaction between the soliton beam and its induced waveguide, we expect that the soliton beam composed of more modes (i.e., more spatially incoherent) should be more stable, since the light intensity will fluctuate more rapidly due to the interference between more modes. This is actually connected to the truth that, for a less spatially coherent beam, it is more difficult to form modulation instability [10].

In conclusion, we have observed that, in order to form partially incoherent optical spatial solitons, the intensity fluctuation of the soliton beam must be much faster than the material can respond to make the material look noninstantaneous. By observing the bicomponent optical spatial solitons, we find that, if the speed of the intensity fluctuation of the soliton beams is much faster than some threshold, the partially incoherent solitons sustain. Otherwise, the light beams go into dynamic soliton-like modes whose behavior is dependent on the speed of their intensity fluctuation.

This research is supported by the National Science Council, Taiwan, under Contract No. NSC-89-2112-M-002-009.

*Electronic address: mfshih@phys.ntu.edu.tw

[1] M. Segev and G. I. Stegeman, Phys. Today **51**, No. 8, 42–48 (1998).
[2] A. W. Snyder *et al.,* Mod. Phys. Lett. B **9**, 1479 (1996).
[3] M. Mitchell *et al.,* Phys. Rev. Lett. **77**, 490 (1996); M. Mitchell and M. Segev, Nature (London) **387**, 880 (1997); Z. Chen *et al.,* Science **280**, 889 (1998).
[4] M. Mitchell *et al.,* Phys. Rev. Lett. **79**, 4990 (1997); M. Mitchell *et al.,* Phys. Rev. Lett. **80**, 5113 (1998); T. Carmon *et al.,* Opt. Lett. **25**, 1113 (2000).
[5] D. N. Christodoulides *et al.,* Phys. Rev. Lett. **78**, 646 (1997); **80**, 2310 (1998).
[6] A. W. Snyder and D. J. Mitchell, Phys. Rev. Lett. **80**, 1422 (1998).
[7] V. V. Shkunov and D. Z. Anderson, Phys. Rev. Lett. **81**, 2683 (1998).
[8] N. Akhmedeiv *et al.,* Phys. Rev. Lett. **81**, 4632 (1998).
[9] M. Segev *et al.,* Phys. Rev. Lett. **73**, 3211 (1994); D. N. Christodoulides and M. I. Carvalho, J. Opt. Soc. Am. B **12**, 1628 (1995).
[10] D. Kip *et al.,* Science **290**, 495 (2000); M. Soljacic *et al.,* Phys. Rev. Lett. **84**, 467 (2000).
[11] M. Shih *et al.,* Opt. Lett. **21**, 931 (1996).
[12] At higher frequency, we do not see this oscillation but only an average intensity because the CCD camera and image analysis system can take pictures at most 15 frames per second.
[13] M. Shih *et al.,* J. Opt. Soc. Am. B **14**, 3091 (1997).
[14] A. W. Snyder *et al.,* Phys. Rev. Lett. **72**, 1012 (1994); Phys. Rev. E **51**, 6297 (1995).
[15] M. Shih *et al.,* Opt. Lett. **21**, 324 (1996); S. Singh *et al.,* Opt. Commun. **118**, 569 (1995).
[16] G. P. Agrawal, *Nonlinear Fiber Optics* (Academic, San Diego, 1995).
[17] The longer propagation requires more time steps to reach steady state. For example, 3600 time steps are required to reach steady state if the propagation length is 15 mm.